A potential explanation for the anomalously low nitrate to phosphate ratio in the well-oxygenated East/Japan Sea

Hyo-Ryeon Kim[1], Jae-Hyun Lim[2], Hae-Kun Jung[3], Jeong-Min Shim[4], Ju-Hyoung Kim[5], Seo-Young Kim[1], and Il-Nam Kim[1,*]

[1]Department of Marine Science, Incheon National University, Incheon, South Korea.
[2]Marine Environmental Research Division, National Institute of Fisheries Science, Busan, South Korea.
[3]Ocean climate and Ecology Research Division, National Institute of Fisheries Science, Busan 46083, South Korea.
[4]Fisheries Resources and Environment Division, East Sea Fisheries Research Institute, National Institute of Fisheries Science, Gangneung 25435, South Korea.
[5]Department of Aquaculture and Aquatic Science, Kunsan National University, Gunsan, South Korea.

Correspondence to: Il-Nam Kim (ilnamkim@inu.ac.kr)

Abstract. The East/Japan Sea (EJS), a well-oxygenated marginal sea, exhibits an anomalously low nitrate (NO_3^-) to phosphate (PO_4^{3-}) ratio (~12.6:1), diverging from the canonical Redfield ratio (16:1). To resolve this long-standing biogeochemical enigma, we examined nitrogen (N) cycling genes and bacterial communities across depths and seasons. External phosphorus inputs—riverine, atmospheric, and crustal—were insufficient to explain the imbalance. Instead, high abundances of N-reducing genes and affiliated taxa suggest a ~~plausible role for~~ widespread potential for bacterially mediated N ~~loss~~reduction throughout the water column. We propose that N removal may occur within particle-associated microenvironments (i.e., oxygen-depleted microzones inside sinking organic aggregates), despite oxygen-rich conditions. A dual-scale feedback—short-term anthropogenic N deposition enriching surface waters (i.e., increasing NO_3^-:PO_4^{3-} ratio in the upper waters) and longer-term deoxygenation, driven by the weakening of deep-water formation, potentially favoring subsurface N loss (i.e., decreasing NO_3^-:PO_4^{3-} ratio in the deep waters)—may promote a vertically stratified NO_3^-:PO_4^{3-} regime in the future EJS. Our findings highlight the EJS as a sentinel system for how combined anthropogenic and climatic forces could reshape marine nutrient balances.

Keywords
East/Japan Sea; Nitrogen cycling; nitrate to phosphate ratio; Redfield ratio; N-reducing genes; Nutrient imbalance; Dual-scale feedback; Anthropogenic and climatic forces

1 Introduction

The biogeochemical cycling of carbon (C), nitrogen (N), and phosphorus (P) in the ocean is tightly linked to phytoplankton growth, which depends on the availability of these essential elements (Arrigo, 2005). The elemental composition of marine organic matter, often described by the Redfield ratio (C:N:P=106:16:1), reflects a global coupling of biological nutrient uptake and remineralization (Redfield, 1958). The similarity between intracellular N:P ratios in phytoplankton and the surrounding seawater's nitrate (NO_3^-) to phosphate (PO_4^{3-}) ratio supports the idea that these elements are consumed and regenerated in near-constant proportions, stabilizing ocean nutrient stoichiometry.

The Redfield N:P ratio of 16:1 is often used to assess nutrient limitation and its effect on primary productivity. On geological timescales, biological dinitrogen (N_2) fixation (N_2 → particulate organic nitrogen; PON) and denitrification (NO_3^- → NO_2^- → N_2O/N_2) act as opposing forces that modulate the ocean's reactive N pool and maintain its global balance (Van Spanning et al.,

2005), referred to as NO_3^-:PO_4^{3-} homeostasis (Gruber, 2008; Tyrell, 1999). These processes are key to regulating nutrient supply, biological productivity, and long-term carbon storage.

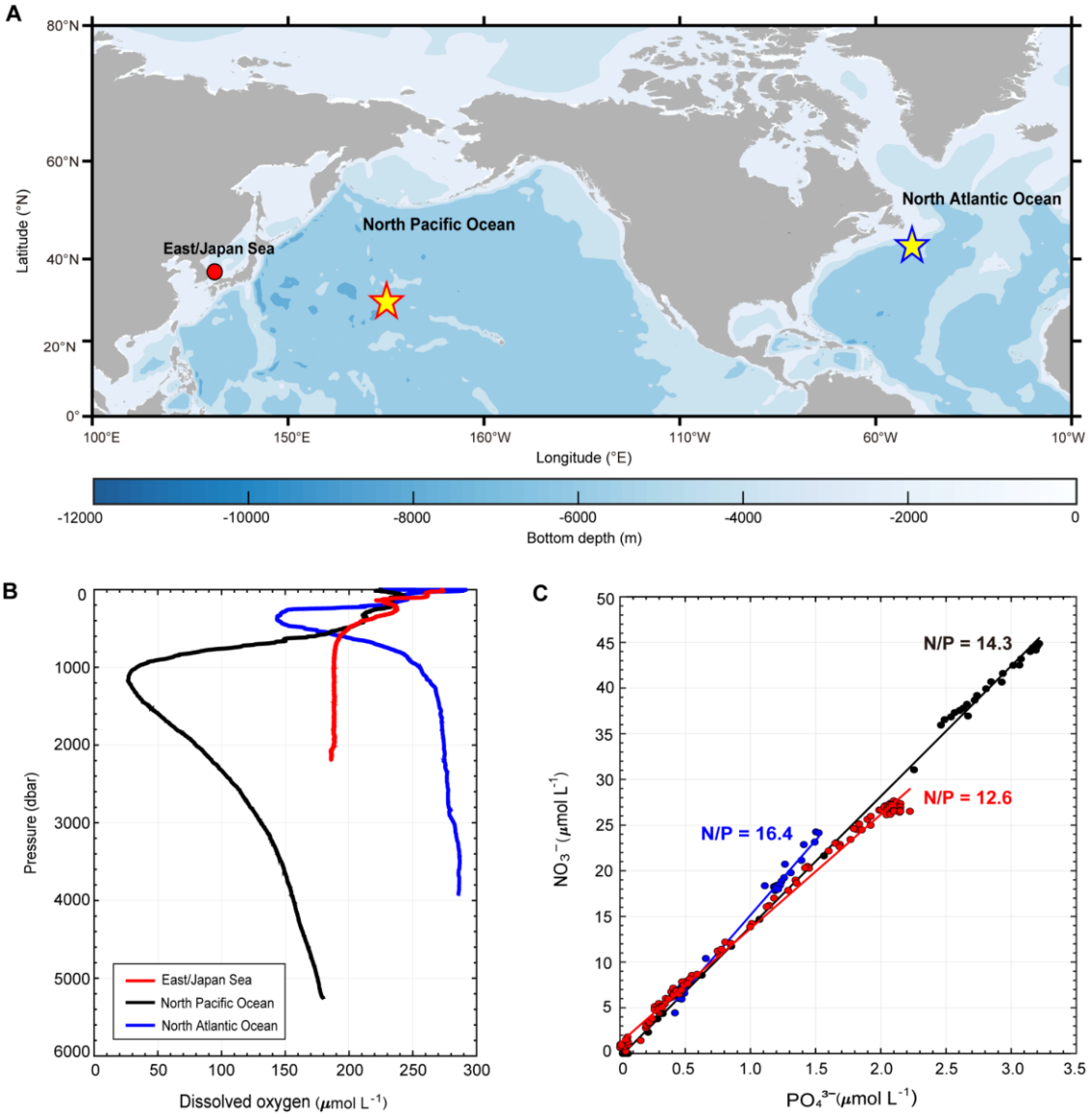

Figure 1: Dual oceanic traits of the East/Japan Sea. The East/Japan Sea (EJS) combines Atlantic-like oxygenation with Pacific-style nitrogen (N) scarcity, revealing a decoupling between redox structure and nutrient stoichiometry. (A) The sampling station in the Ulleung Basin, EJS (filled red circle), and reference stations in the North Pacific Ocean (NPO) and North Atlantic Ocean (NAO) (red- and blue-edged stars, respectively) are shown at comparable latitudes. (B) Vertical profiles of dissolved oxygen (µmol L^{-1}), and (C) NO_3^-: PO_4^{3-} ratios, are presented for each basin. Solid black, blue, and red lines represent the NPO, NAO, and EJS stations, respectively (This plot shows strong linear correlations in the NPO ($R^2 = 0.96$, $p < 0.05$), NAO ($R^2 = 0.95$, $p < 0.05$), and EJS ($R^2 = 0.92$, $p < 0.05$)). To contextualize the EJS biogeochemistry, DO, NO_3^- and PO_4^{3-} data from the ES were compared with reference profiles from station 76 (P02 section, North Pacific) and station 12 (A20 line, North Atlantic), retrieved from the CLIVAR and Carbon Hydrographic Data Office (CCHDO; https://cchdo.ucsd.edu).

Although the global NO_3^-:PO_4^{3-} ratio closely aligns with the Redfield ratio, significant regional deviations are widely observed in the ocean~~exist~~ (Gruber, 2008; Martiny et al., 2013) (Fig. 1A). For instance, in the North Atlantic Ocean (NAO), where deep convection and high oxygen concentrations prevail, the NO_3^-:PO_4^{3-} ratio exceeds 16:1, likely reflecting elevated N_2 fixation (Gruber and Sarmiento, 1997) (Fig. 1B and 1C). Conversely, in the North Pacific Ocean (NPO), which represents the terminal region of the global overturning circulation and contains relatively old deep waters with lower~~where circulation terminates and~~ oxygen concentrations~~ are low~~, denitrification reduces the N inventory (Deutsch et al., 2001), leading to a lower NO_3^-:PO_4^{3-} ratio of ~ 14.3:1 (Fig. 1B and 1C). These variations highlight the regional imprint of biogeochemical processes on nutrient distributions.

The East/Japan Sea (EJS), a marginal sea in the northwest Pacific (~~Supplementary~~ Fig. S1), is characterized by active deep-water formation and strong thermohaline circulation, frequently referred to as a 'Miniature Ocean' (Seung and Yoon, 1995). Despite its well-oxygenated conditions–comparable to those in the NAO–the EJS displays a remarkably low NO_3^-:PO_4^{3-} ratio of 12.6:1, lower even than that of the NPO (Fig. 1B and 1C). Large-scale hydrographic surveys conducted through the CREAMS and ONR JES programs (1998–2000) first established the anomalously low NO_3^-:PO_4^{3-} ratios in the EJS, with basin-wide estimates of 11.2 ± 3.9 (summer 1999) and 12.6 ± 0.6 (winter 2000), consistently below the canonical Redfield ratio (Kim et al., 2012). Subsequent compilations, including historical datasets, have confirmed this feature across the basin, with reported range from ~ 11.4 to 14.7 (Lee and Rho, 2015), consistently below the canonical Redfield ratio (16:1), with the lowest estimate (~ 11.4) derived from historical datasets compiled by Yanagi (2002). Previous studies have attributed the low NO_3^-:PO_4^{3-} ratios in the EJS to a combination of physical circulation and remineralization (Kim and Kim, 2013), inflow of low NO_3^-:PO_4^{3-} waters from the East China Sea (Lee et al., 2007), and possible denitrification (Yanagi, 2002); however, definitive evidence explaining how such low ratios are maintained in this well-oxygenated basin remains limited~~While some studies have proposed that denitrification might contribute to N loss in the EJS, definitive evidence is still lacking~~ (Kim et al., 2012; Kim, 2015; Na et al. 2018). Consequently, the anomalously low NO_3^-:PO_4^{3-} ratio in the EJS has long remained a scientific enigma.

Much of our current understanding of marine N cycling has historically relied on~~derives from~~ cultivation-based studies and stable isotope analyses conducted across diverse marine environments. While these approaches have yielded important insights into microbial identities and transformation rates (Marchant et al., 2016), they are limited by the low cultivability of many marine microbes and the complex interpretation of isotopic data (Pace, 1997). Advances in molecular techniques, particularly 16S rRNA-based metagenomics, now enable the targeted use of bacterial biomarker genes to elucidate N cycling processes in marine environments (Bao et al., 2025; Biao et al., 2025; Delmont et al., 2022; Ding and Sun, 2025; Lüke et al., 2016; Pajares and Ramos, 2019; Sharma et al., 2014). However, studies directly examining N cycling processes in the EJS remain limited, particularly those integrating genomic approaches capable of resolving microbial functional potential.

Here, we present the first attempt to uncover potential clues to the anomalously low NO_3^-:PO_4^{3-} ratio in the well-oxygenated EJS, using bacterial biomarker genes and community compositions involved in N cycling. To this end, we conducted a research cruise in 2021, collecting water samples from five depths (0, 150, 300, 750, and 1000 m) over five months (February, April, June, August,

and October). Our findings offer novel insights into microbial N cycling in well-oxygenated waters and contribute to resolving a long-standing biogeochemical enigma in the EJS.

2 Materials and Methods

2.1 Sampling and measurements of physical and biogeochemical parameters

Seawater samples for sequencing and physicochemical analysis were collected in the Ulleung Basin (UB) of the East Sea aboard R/V Tamgu 3 from February to October 2021 (Fig. 1A and ~~Supplementary~~ Fig. S1). Vertical profiles of temperature (T), salinity (S), and dissolved oxygen (DO) were measured from the surface (0m) to 1000 m using a Sea-Bird SBE 911plus CTD system equipped with a rosette sampler. Sensor accuracies were ± 0.001 °C for T, ± 0.0003 S m^{-1} for conductivity, and ± 2% for DO. Seawater samples for nutrients (NO_3^- and PO_4^{3-}) analyses were collected in acid-rinsed 15 mL vials and frozen at −20 °C. Nutrient concentrations were determined using a QuAAtro autoanalyzer (Seal Analytical, Germany) with analytical precision within 1%. For DNA extraction, 2L of surface seawater was filtered through 0.22 μm cellulose ester membrane filters (Millipore, Ireland) to capture bacterial cells. Filter~~sed samples~~ were immediately frozen and subsequently stored at −80°C until DNA extraction.

2.2 Bacterial community composition and biomarker gene analysis

Genomic DNA was extracted from ~~2L of seawater filtered through~~ 0.22 μm cellulose ester membrane~~s~~ filters (Millipore, Ireland) onto which 2L of seawater had been filtered (Fuhrman et al., 1988). Total DNA was isolated using a DNA isolation kit (Qiagen, Germany) following the manufacturer's protocol, and the quality of the extracted DNA was verified with a NanoDrop spectrophotometer (Thermo Scientific, USA) (Desjardins and Conklin, 2010). After quality control,

16S rRNA sequencing libraries were constructed according to the Illumina 16S Metagenomic Sequencing Library Preparation protocol (Illumina, San Diego, CA, USA), targeting the V3–V4 hypervariable regions of the 16S rRNA gene (Klindworth et al., 2013). PCR amplification was performed with primers containing Illumina overhang adapters (Forward: 5′-TCGTCGGCAGCGTCAGATGTGTATAAGAGACAGCCTACGGGNGGCWGCAG-3′; Reverse: 5′-GTCTCGTGGGCTCGGAGATGTGTATAAGAGACAGGACTACHVGGGTATCTAATCC-3′;). The extracted DNA samples were sequenced on the Illumina MiSeq platform (2 × 300 bp paired-end, v3 chemistry) using MiSeq Control Software (v2.4.1.3) and Real-Time Analysis (RTA v1.18.54.0) (Kozich et al., 2013). Library preparation included limited-cycle PCR, indexing, normalization, and pooling, and 16S tagging of DNA fragments (100–300 bp) was performed using a quantitative DNA library preparation kit. Raw sequencing data were processed using QIIME 1.9.1, wherein paired-end reads were assembled into tags based on their overlapping regions. During the preprocessing stage, primers were trimmed, followed by demultiplexing and quality filtering (Phred ≥ 20). USEARCH7 was employed for denoising and chimera detection/filtering in operational taxonomic units (OTUs) clustering process. Then, OTUs were then assigned using the Silva132 and NCBI databases (Sayers et al. 2021; Quast et al., 2013), with a 97% sequence similarity threshold via UCLUST and a close-reference clustering approach (Edgar, 2010). OTU identifiers were established accordingly. The resulting OTU table was normalized by dividing each OTU count by the corresponding

16S rRNA gene copy number abundance. The filtered OTU table, in BIOM (Biological Observation Matrix) format, was subsequently clustered using the PyNAST (Python Nearest Alignment Space Termination) algorithm, applying a 97% similarity threshold. Taxonomic classification was conducted across multiple hierarchical levels, Phylum, Class, Order, Family, Genus, and Species, using the RDP classifiers. The relative abundance of phyla, classes, orders, families, genera, and species was estimated using the STAMP (Statistical Analysis of Metagenomic Profiles) program. Relative abundances of bacterial taxa were calculated as read counts normalized by predicted 16S rRNA gene copy number. In this study, bacterial community composition was analyzed at the order level. Functional profiling of bacterial sequences was performed using Tax4Fun2 (Wemheuer et al., 2020), a computational tool that infers functional attributes of bacterial communities from 16S rRNA gene data, leveraging the Ref99NR reference genome data base. Functional annotations were derived through comparison with Kyoto Encyclopedia of Genes and Genomes (KEGG) Orthology reference matrices from the KEGG database. The generated 16S rRNA sequence data have been deposited in the NCBI Sequence Read Archive (accession number: PRJNA1168283 and PRJNA1253365). The gene abundance and taxonomic composition (OTU counts) used in this study are based on relative, rather than absolute, measurements across samples. Accordingly, these data are most suitable for assessing vertical and seasonal variations in community structure and functional potential, but do not provide direct quantitative estimates of N loss rates.

3 Results and Discussion

3.1 Vertical structure and stoichiometry of NO_3^- and PO_4^{3-} in the East/Japan Sea

Depth-resolved profiles of NO_3^- and PO_4^{3-} obtained during five cruises in 2021 reveal a vertically structured yet temporally consistent distribution across the full water column (0–1000 m; Fig. 2A and 2B). Surface waters (0 m) exhibited low concentrations of both NO_3^- (0.69–4.95 μmol L^{-1}) and PO_4^{3-} (0.004–0.27 μmol L^{-1}), which increased with depth, thereby forming a pronounced gradient between 100 and 500 m (NO_3^-: 6.33–26.65 μmol L^{-1} and PO_4^{3-}: 0.41–1.99 μmol L^{-1}). At depths of 750–1000 m, both NO_3^- and PO_4^{3-} converged to a narrow range (NO_3^-: 26.67–27.39 μmol L^{-1}; PO_4^{3-}: 2.00–2.09 μmol L^{-1}), with minimal variability across depths and seasons, indicating a stable deep-water distribution. Building on this vertical structure, NO_3^-:PO_4^{3-} ratios provide a more integrative constraint on nutrient stoichiometry by linking the relative availability of NO_3^- and PO_4^{3-} across depths (Fig. 2C). Surface NO_3^-:PO_4^{3-} ratios were highest in February, reaching 18.64, consistent with elevated nutrient concentrations. In the upper ~300 m, ratios exhibited seasonal variability but remained generally below the canonical Redfield ratio (16:1), with only occasional exceedances at 20–30m in August (20.51) and October (28.99). With increasing depth (between 300–1000 m), this variability became constrained, and ratios consistently converged to a narrow range of 12.97–14.32 across all sampling periods, indicating a persistent and depth-invariant stoichiometric structure (to avoid artificial inflation under near-detection-limit conditions, ratios were calculated excluding samples with PO_4^{3-} < 0.05 μmol L^{-1}). Accordingly, this depth-dependent convergence demonstrates that deviations from Redfield stoichiometry are not random but systematically structured across the entire water column. To further assess whether the low NO_3^-:PO_4^{3-} signature reflects a consistent, water column–integrated feature, we examined the relationship between NO_3^- and PO_4^{3-} across all depths (Fig. 2D). Slopes of the NO_3^-– PO_4^{3-} regressions ranged from 12.7 in February to 13.0–

13.2 during April, June, August, and October, with only minor seasonal variation. All slopes remained well below the canonical Redfield ratio (16:1), thereby demonstrating that the low NO_3^-: PO_4^{3-} signature is consistently maintained across the entire water column and throughout the sampling period. The close agreement between depth-resolved ratios and bulk relationships demonstrates that the low NO_3^-:PO_4^{3-} signature a coherent, water column scale feature that persists across sampling periods, rather than arising from localized or transient conditions.

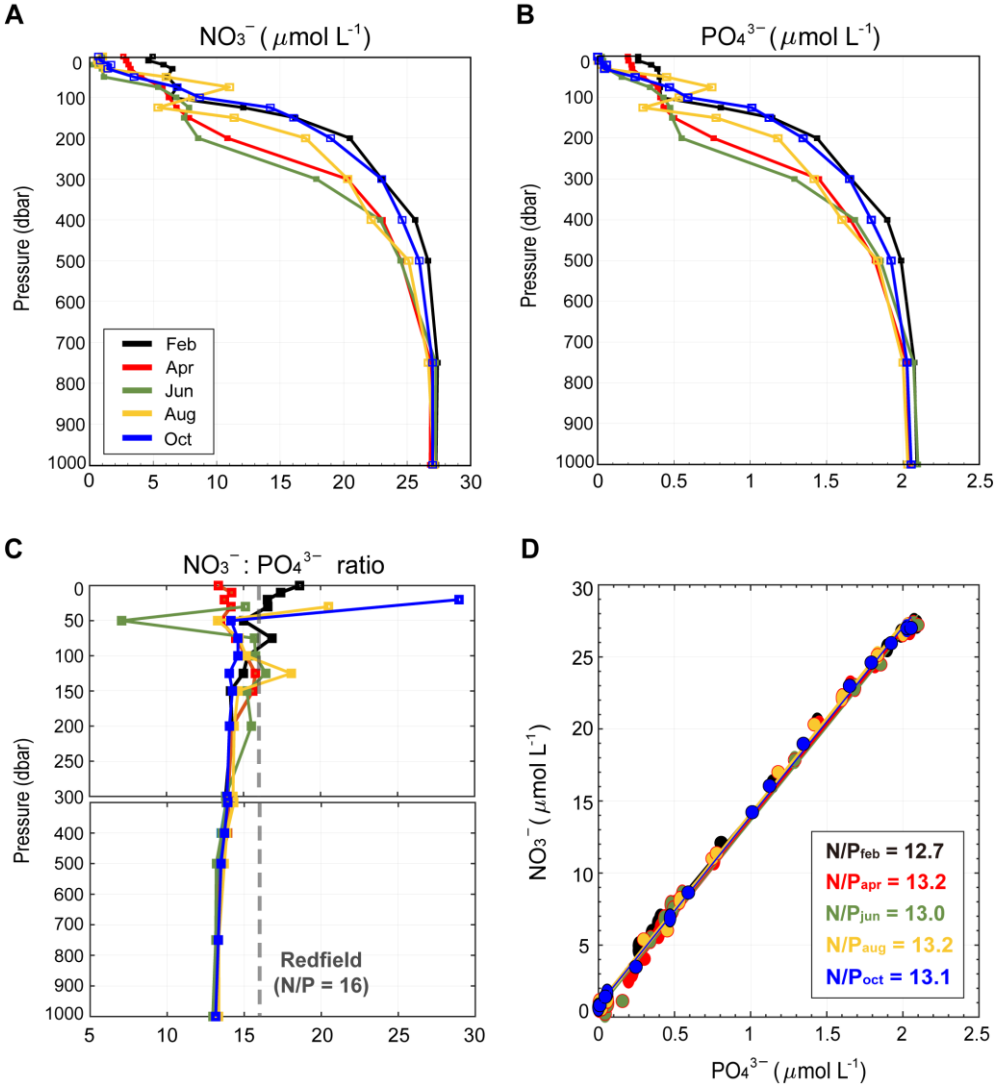

Figure 2: Vertical nutrient structure and stoichiometry in the EJS 2021. Depth profiles of (A) NO_3^- and (B) PO_4^{3-} concentrations (µmol L^{-1}), (C) NO_3^-:PO_4^{3-} ratios across five cruises conducted in February (black), April (red), June (green), August (yellow), and October (blue), spanning 0–1000 m. The ratio profiles in (C) were calculated excluding samples with PO_4^{3-} concentrations below 0.05 < µmol L^{-1} to avoid artificial inflation under low- PO_4^{3-} conditions, following common practices in marine stoichiometric analyses. The dashed gray line indicating the canonical Redfield ratio (16:1). (D) Scatter plot of PO_4^{3-} versus NO_3^- concentrations for all months and depths.

~~**3.1 External phosphorus inputs are insufficient**~~

~~The anomalously low NO_3^-:PO_4^{3-} ratio in the EJS may result from either an excess P supply or N loss. To assess the former, we evaluated all plausible external P sources, including riverine discharge, atmospheric deposition, and seawater–crust interaction.~~

~~First, riverine discharge is a recognized vector for both particulate and dissolved P in marine environments (Withers and Jarvie, 2008). However, the EJS lacks major river systems capable of supplying significant P at the basin scale. In particular, discharge from Nakdong River—the most prominent riverine source in the region—is limited by the construction of a dam at its estuary (June 1990) and exhibits a low flow rate (mean: ~0.0004 Sv; 1 Sv = 10^6 m^3 sec^{-1}) (Yang et al., 2002). A seasonal alternative is the intrusion of Changjiang Discharge Water (CDW) from the East China Sea, which enters the southern EJS during summer (Supplementary Fig. S2) (Isobe et al., 2002). While the CDW may contain P, it is relatively enriched in N and confined to surface layers (Tseng et al., 2014). Furthermore, its influence has likely declined due to decreasing discharge volume (Myriokefalitakis et al., 2016). Together, these factors indicate that riverine P input to the EJS is spatially constrained, temporally limited, and minor in magnitude relative to N.~~

~~Second, atmospheric deposition can also contribute bioavailable P to surface waters via aerosols, mineral dust, and volcanic ash (i.e., particularly in regions influenced by volcanic activity) (Myriokefalitakis et al., 2016). The EJS lies downwind of heavily industrialized and densely populated areas of Northeast Asia, making it a potential recipient of anthropogenic emissions (Seo and Kim, 2023). However, recent studies have shown that since the 1980s, atmospheric deposition has led to a substantial increase in reactive N in the upper EJS (~0.24 μmol kg^{-1} yr^{-1}), resulting in a measurable rise in NO_3^- relative to PO_4^{3-} concentrations (Kim et al., 2014). This N-enriched atmospheric deposition can be excluded as a significant P source.~~

~~Lastly, seawater–crust interactions, particularly at hydrothermal vents under low-oxygen and high-temperature conditions, are known to release PO_4^{3-} into the water column (McManus et al., 1997). However, no hydrothermal activity has been identified within the EJS.~~

~~Taken together, these findings indicate that none of the plausible external P sources—riverine input, atmospheric deposition, or seawater–crust interaction—are sufficient to account for the anomalously low NO_3^-: PO_4^{3-} ratio observed in the EJS. Thus, increased P supply is unlikely to be the primary driver of the long-standing NO_3^-: PO_4^{3-} anomaly in the EJS.~~

3.2 Genetic and taxonomic evidence for N loss

~~Given that external P inputs are insufficient to explain the anomalously low NO_3^-: PO_4^{3-} ratio in the EJS, we next consider an alternative mechanism~~Motivated by this observation, we focus on internal ~~:~~N loss ~~via~~mediated by bacterial~~ly mediated~~ processes within water column. In the marine N cycle, N loss is primarily driven by two bacterial pathways: NO_3^- reduction ($NO_3^- \xrightarrow[nap,\ nar]{} NO_2^-$) (Moreno-Vivián et al., 1999), and denitrification ($NO_3^- \xrightarrow[nap,\ nar]{} NO_2^- \xrightarrow[nir]{} NO \xrightarrow[nor]{} N_2O \xrightarrow[nos]{} N_2$) (Hallin et al., 2018). These processes are catalyzed by key biomarker genes, including *nar*, *nap*, *nor*, *nir*, and *nos* (hereafter referred to as N-reducing genes; Fig. ~~2A~~3A).

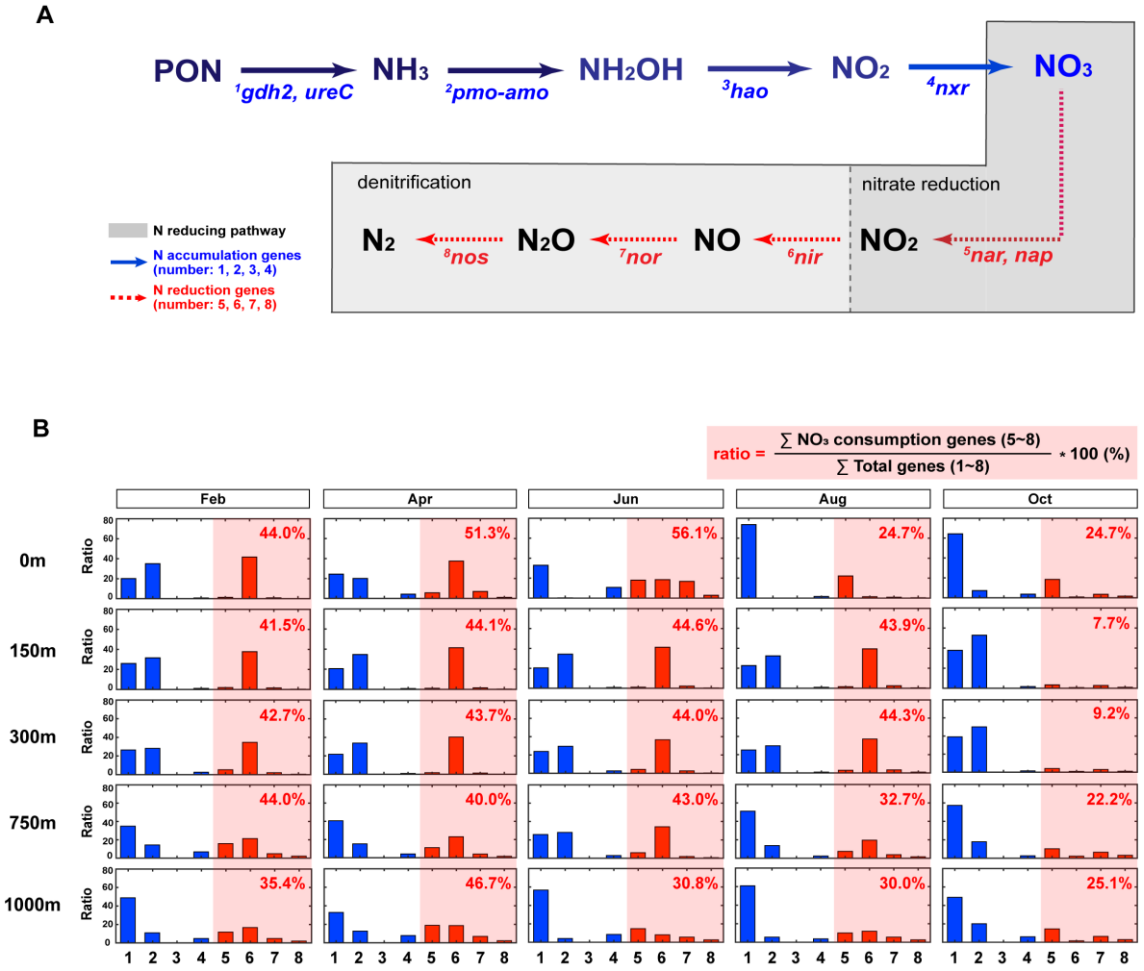

Figure 32: Temporal and depth-resolved structuring of nitrogen (N) reducing genes. (A) Blue solid arrows represent N-accumulation pathways, with associated genes (1–4) labeled beneath each arrow. In contrast, red dashed arrows indicate N reducing pathways, involving genes 5–8. Among these, NO_3^- nitrate reduction and denitrification—two major N-reducing pathways—are grouped within gray-shaded boxes. (B) The relative contribution of each N transformation step (genes 1–8; panel A) is expressed as a percentage of the total N-cycling gene pool for each cruise-depth sample. Blue bars denote N accumulation–associated genes, whereas red bars denote N reduction–associated genes. Values shown within the red-shaded boxes indicate the percentage contribution of NO_3^- reduction and denitrification–associated genes (*nar*, *nap*, *nir*, *nor*, and *nos*) relative to the total N transformation gene pool, including all genes involved in ammonification, nitrification, and denitrification. Each bar represents a single observation; error bars are not shown.

We quantified the relative abundance (%) of To identity the extent of N-reducing bacterial taxa associated with N-reduction pathways and characterized the distribution of bacterially mediated N-reducing genes loss (i.e., N sinks), we analyzed the abundance of N-reducing genes and their associated bacterial communities across five depths (0, 150, 300, 750, and 1000 m) and five months (February, April, June, August, and October) in the EJS. The relative proportion (%) of potential N-reducing genes (*nar*, *nap*, *nir*, *nor*, and *nos*) was calculated as their fraction within the total N transformation gene pool, defined to include all annotated genes associated with ammonification, nitrification, and denitrification, (defined here as all analyzed N-cycling pathways including

~~ammonification, nitrification, and denitrification genes)~~ and exhibited pronounced vertical and seasonal variability (Fig. 3~~2~~B). From February to June, N-reducing genes accounted for 44.0–56.1% of the total N genes at the surface, decreasing steadily with depth to a minimum of 30.8% at 1000m. In August, surface abundance declined to 24.7%, while mid-depth layers (150–300m) showed elevated values of 43.9–44.3%, and deep layers (750–1000m) maintained moderate levels (30.0–32.7%). By October, ~~abundances~~ proportions declined across all depths, with mid-depth values decreasing to~~reaching~~ 7.7–9.2%~~ at mid-depth~~. In contrast, deep layers remained relatively stable, ranging from ~~-~~22.2–25.1% throughout the study period ~~Temporal variability was particularly prominent at the surface and mid-depth layers, while the deep layers remained relatively stable (22.2–25.1%)~~ (~~Supplementary~~ Table S1).

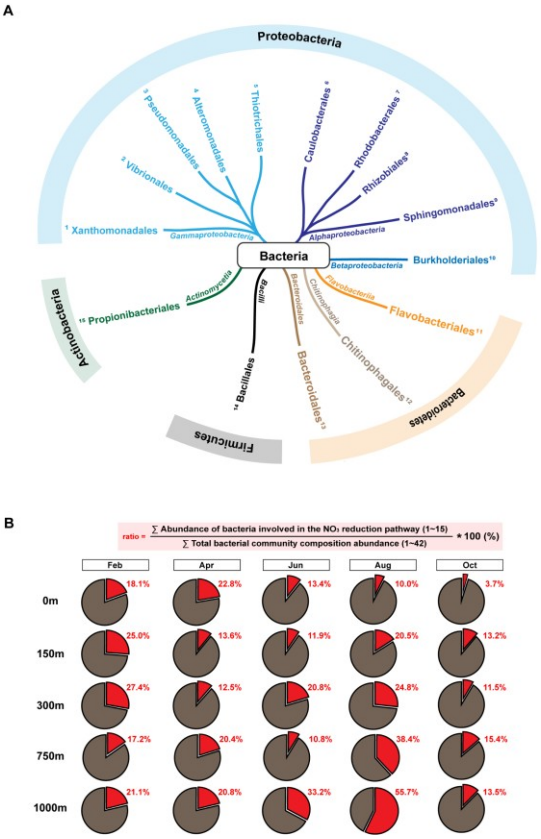

Figure 4~~3~~: Spatiotemporal distribution of functionally grouped N-reducing bacterial communities. (A) Radial tree diagram showing the phylogenetic distribution of the ~~for N-reducing~~ 15 bacterial orders classified as N-reducing groups among the 42 bacterial orders detected in the East/Japan Sea. These 15 orders were selected based on previously reported metabolic capabilities associated with N reduction pathways (e.g., NO_3^- reduction and denitrification). Node color~~s~~ represent class-level taxonomy, while node numbers (1–15) indicate bacterial orders functionally classified as N-reducing. (B) Relative contribution of ~~Proportion of~~ N-reducing bacterial groups across samples, calculated as the fraction of OTU counts assigned to ~~cumulative abundance of~~ the 15 orders of N-reducing taxa ~~in (A),~~ relative to the total OTU counts of ~~abundance of~~ all 42 detected bacterial orders ~~identified~~ in ~~this study~~each sample. This portion is represented by the red segment of ~~The resulting ratio is shown as a red-colored segment in~~ each pie chart, with numerical values indicating the corresponding percentage~~annotated accordingly~~.

~~We further examined the~~ The relative contribution~~abundance~~ (%) of N-reducing taxa was calculated as the fraction of OTUs affiliated with taxonomic lineages known to possesses and perform N-reducing pathways relative to the total detected bacterial taxa

at the order level in the EJS. ~~bacterial taxa at the order level that are potentially involved in N removal~~ (hereafter referred to as N-reducing bacterial taxa) (Fig. ~~4~~3). Of the 42 bacterial orders identified in the EJS (~~Supplementary~~ Table S2), 15 were associated with N reduction pathways: three primarily associated with NO_3^- reduction (*Flavobacteriales*, *Caulobacteriales*, and *Thiotrichales*) (Starke et al., 2017), and twelve functionally linked to denitrification (*Rhodobacteriales*, *Alteromonadales*, *Pseudomonadales*, *Burkholderiales*, *Propionibacteriales*, *Bacillales*, *Rhizobiales*, *Chitinophagales*, *Bacteroidales*, *Vibrionales*, *Sphingobacteriales*, and *Xanthomonadales*) (Fujii et al., 2022; Podlesnaya et al., 2020; Russell et al., 2024; Starke et al., 2017; Wang et al., 2018; Wei et al., 2019; Wu et al., 2022) (Fig. ~~3~~4A). In February, abundance increased with depth, from 18.1% at the surface to a maximum of 27.4% at 300 m, decreasing thereafter to 17.2–21.1% at 750–1000 m (Fig. ~~3~~4B). In April, the opposite pattern emerged: surface abundance peaked at 22.8%, declining to 12.5% at 300 m, and stabilizing at 20.4–20.8% at deep layers. In June, abundance ranged from 10.8% to 20.8% between 0 and 750 m, followed by a sharp increase to 33.2% at 1000 m. In August, the lowest surface value (10.0%) ~~coincided with a progressive increase with depth, culminating in the highest observed value~~ and increased progressively with depth, reaching a maximum of ~~(~~55.7%~~)~~ at 1000 m, indicating a clear depth-dependent pattern. In contrast, October exhibited uniformly low abundances throughout the water column (3.7–15.4%), consistent with the distribution of N-reducing genes (~~Supplementary~~ Table S3). The N-reducing bacterial orders identified in this study are not region-specific but belong to widely distributed heterotrophic groups consistently linked to organic matter degradation and particle-associated lifestyles. Notably, taxa such as *Alteromonadales*, *Flavobacteriales*, *Burkholderiales*, *Rhizobiales*, *Rhodobacterales*, and *Oceanospirillales* have been shown to preferentially utilize particulate or semi-labile organic matter and to respond to organic nutrient pools (e.g., DON, DOP), highlighting their central role in marine biogeochemical cycling (Fontanes et al., 2015; Kong et al., 2021; Quan et al., 2024). The recurrence of these functionally characterized taxa in our dataset, together with their vertical co-occurrence with NO_3^- reduction–associated genes, points to a conserved ecological linkage rather than a regionally unique assemblage. Their persistent occurrence across the full water column is not unique to this system, but reflects a broadly conserved ecological pattern observed across diverse marine environments. In particular, their known association with particle-rich microenvironments provides a mechanistic basis for this pattern, as such niches can sustain localized oxygen depletion through intensified microbial respiration. This framework explains how NO_3^- reduction and denitrification can occur within an otherwise well-oxygenated water column, linking microbial community structure to N-reducing processes across depth. The consistent presence of these taxa therefore supports a particle-mediated pathway for N loss, reinforcing the interpretation that the observed low NO_3^-:PO_4^{3-} signature reflects an internally sustained, water column integrated process.

Overall, the mean proportions of N-reducing genes and their affiliated taxa across the study period were 37.7% and 20.0% ~~(Supplementary Fig. S3)~~, respectively, indicating the potential for bacterially mediated N loss in the EJS water column (Fig. S3). ~~As the actual rates of N loss via these pathways were not directly quantified, the study has limitations in quantitative interpretation. However, the combined gene and taxonomic evidence suggests that bacterially mediated N loss may contribute to the anomalously low NO_3^-: PO_4^{3-} ratio in the EJS.~~While these estimates do not directly quantify N-loss rates, previous work has demonstrated that functional gene abundance can be positively associated with process rates across diverse ecosystems, suggesting that gene-based

metrics can capture ecologically meaningful variation in biogeochemical potential (Rocca et al., 2015). In this context, the observed proportion of NO_3^- reduction–associated genes (37.7%) and taxa (20.0%) observed here indicates that the potential for bacterially mediated N loss in the EJS water column is unlikely to be negligible. Consistent with this interpretation, NO_3^--reduction genes have been repeatedly detected in oxygenated marine environments. For example, metagenomic and particle-associated studies have identified these genes (e.g., *nir*, *nar*), along with their affiliated microbial taxa, as a persistent component of microbial assemblages throughout oxic water columns, from surface to deep waters, even under fully oxygenated and strongly mixed conditions in the western subarctic Pacific (Li et al., 2018). Similarly, *nir* genes, dominated by *nirS*, were consistently detected across all samples (n = 107) spanning multiple depths along the Pacific coastal zone of China, where their total abundance exceeded that of ammonia-oxidation genes (*amoA*) (Wan et al., 2023). A greater abundance of *nir* genes relative to *amo* genes has also been widely reported in eutrophic estuaries, suggesting elevated N-reduction potential in these highly perturbed coastal systems (Dai et al., 2022; Tang et al., 2022; Zhang et al., 2014). In addition, metagenomic analyses from a hypereutrophic lagoon showed that dissimilatory NO_3^- reduction to ammonium (DNRA) and denitrification were active even under fully oxygenated conditions (> 224 μM), accounting for approximately one-fifth of total N recycling processes (Broman et al., 2021). Although most studies do not report directly comparable normalized abundances, these results collectively indicate that NO_3^- reduction genes typically represent a non-negligible fraction of N cycling functional potential in oxic systems. Taken together, these studies indicate that NO_3^- reduction genes in oxic systems are typically present but limited in distribution and relative contribution, in contrast to the substantially higher and vertically persistent proportions observed here. However, direct numerical comparison remains inherently constrained by differences in gene normalization, sequencing depth, and ecosystem structure. Rather than enabling strict cross-system equivalence, these contrasts highlight a key implication: the EJS water column sustains a comparatively elevated and vertically integrated reservoir of N-reduction functional potential under fully oxygenated conditions. In this sense, our results move beyond site-specific observations to define a quantitative, depth-resolved baseline for N reduction potential in oxic marine systems, providing a reference framework for future comparative and process-based studies.

3.3 How can N loss proceed in oxygenated waters?

The widespread occurrence of NO_3^- reduction associated genes and taxa identified above implies that N loss processes are not restricted to localized or transient conditions in the EJS. Despite the well-oxygenated condition of the EJS water column (O_2 > 180 μmol L^{-1}; Fig. 1B), several characteristics of the system provide a plausible physical and biogeochemical context for sustaining such processes~~., our results suggest that N loss processes are likely to occur throughout the water column. This paradox may be reconciled by particle-associated microenvironments (i.e., oxygen-depleted microzones within sinking aggregates).~~ A key feature of the ~~The~~ EJS is the combination of ~~combines~~ high primary production with efficient vertical export, which promotes the formation of ~~producing~~ large, fast-sinking, and highly porous aggregates and fecal pellets (Kwak et al., 2013; Otosaka et al., 2008). Within these particles, heterotrophic respiration consumes O_2 faster than it is replenished by diffusion, leading to steep O_2 gradients and

suboxic–anoxic interiors at the millimeter scale, even while surrounding waters remain oxygenated (Alldredge and Cohen, 1987; Ploug et al., 1997). These particle-associated microenvironments provide a physically plausible setting for NO_3^- reduction and denitrification to occur within the water column. While ~~P~~previous studies have reported that benthic denitrification have also been detected along the Ulleung Basin margin (Kim et al., 2012; Na et al., 2018)~~. However, the~~ estimated ~~benthic denitrification~~ rates are ~~were~~ insufficient to explain the persistently low basin-scale NO_3^-: PO_4^{3-} ratio in the EJS, indicating that additional N loss pathways in water column are required~~, such as particle-associated microenvironments, are likely involved~~. In the light of these considerations, the particle-associated microenvironment mechanism described here is not specific to the EJS, but has been repeatedly supported by theoretical, modelling, and observational studies across diverse marine environments. Global syntheses and modeling ~~further~~ demonstrate~~show~~ that such microenvironments extend the ecological niche for anaerobic metabolisms well beyond oxygen-minimum zones (OMZs) (Bianchi et al., 2018), resulting in the occurrence of N-loss pathways such as NO_3^- reduction and denitrification inside aggregate interiors (Alldredge and Silver, 1988). ~~High abundances of N-reducing genes and taxa observed in the EJS are consistent with these mechanisms.~~

Empirical support for particle-associated N loss under oxygenated conditions has been reported across a range of marine environments. In the eastern tropical North Pacific, laboratory incubations and field observations directly showed denitrification within slowly sinking diatom aggregates in oxic seawater (Ciccarese et al., 2023). In the northeast Pacific, aggregate-associated NO_3^- respiration and denitrification were measured in oxygenated bottom waters (O_2 > 100 μmol L^{-1}), particularly during periods of elevated particle flux (Wolgast et al., 1998). Independent isotopic evidence likewise indicated denitrification within particle-associated microenvironments in oxygenated waters of the subtropical and temperate North Pacific (Yamagishi et al., 2005). Additional observations from the South Pacific subtropical gyre and oxygenated estuary–shelf systems further suggest that particle-associated microzones can sustain NO_3^- reduction beyond classically oxygen-deficient settings (Kim et al., 2013; Wan et al., 2023). Collectively, these studies indicate that particle dynamics can decouple bulk-water oxygen conditions from microscale N transformations. Against this background, the seasonal and vertical variability observed in the EJS can be interpreted as the outcome of coupled physical and biogeochemical controls. Seasonal stratification and winter mixing regulate nutrient resupply and upper-water-column production, thereby controlling both the magnitude and vertical export of particulate organic matter. During stratified periods, reduced vertical mixing and enhanced surface production can promote the accumulation and downward transport of organic particles, whereas winter mixing redistributes nutrients and particles throughout the water column. The subsequent degradation and remineralization of these particles can generate localized microenvironments that favor NO_3^- reduction even when the surrounding water remains oxygenated, linking seasonal physical forcing to depth-dependent variability in N cycling (Cram et al., 2015; Loisel et al., 2002; Wakeham and Lee, 1993). The depth-dependent and seasonally modulated N:P patterns observed here are therefore consistent with the possibility that N loss is not confined to canonical oxygen-deficient zones, but may occur episodically within particle-associated microenvironments across the oxic water column. In this context, the widespread occurrence of nitrate-reduction–associated genes and taxa throughout the water column supports a persistent nitrogen-reducing potential and provides a plausible mechanistic link between environmental variability and the formation and maintenance of low NO_3^-:PO_4^{3-} ratios in the EJS.

~~Similar cases of N loss in oxygenated waters have been reported across marine environments, particularly in (i) the eastern tropical North Pacific (ETNP), where laboratory experiments and a transect study showed denitrification within slowly sinking diatom aggregates in oxygenated seawater (Ciccarese et al., 2023); (ii) the northeast Pacific, where aggregate-linked NO_3^- respiration and denitrification were directly measured in oxygenated bottom waters (O_2 > 100 μmol L^{-1}), particularly during periods of high particle flux (Wolgast et al., 1998); (iii) the subtropical/temperate North Pacific, where N_2O isotopomer signatures detected in oxygenated waters are consistent with denitrification occurring within particle-associated microenvironments (Yamagishi et al., 2005); (iv) the South Pacific subtropical gyre, where basin-scale analyses along 32°S revealed measurable denitrification signals within the oxygen minimum layer (1100–2000 m), suggesting that particle-associated microzones may sustain N loss processes even in well-oxygenated open-ocean waters (Kim et al., 2013); and (v) oxygenated estuary–shelf waters of the Pearl River, Jiulong River, and Changjiang systems, where size-fractionated incubations implicate denitrification on larger particles as a dominant N_2O source (Wan et al., 2023). Our findings in the EJS align with these observations, indicating that oxygenated water columns do not necessarily preclude N removal—especially where and when particle-associated microenvironments exist.~~

3.4 External phosphorus inputs cannot explain the low NO_3^-:PO_4^{3-} ratios

Any mechanism capable of explaining the anomalously low NO_3^-:PO_4^{3-} ratios in the EJS must be able to sustain this signal across the water column. This constraint reduces the problem to two possibilities—enhanced P supply (source) or net N removal (sink); while the latter is addressed in Sections 3.2–3.3, here we test the former. In this 3.4 section, we evaluate whether external P inputs satisfy this requirement by systematically assessing all plausible P sources to the basin.

First, riverine discharge is a recognized vector for both particulate and dissolved P in marine environments (Withers and Jarvie, 2008). However, the EJS lacks major river systems capable of supplying significant P at the basin scale. The Nakdong River, the most prominent riverine source to the southern EJS, has been regulated by and estuarine barrage constructed in 1990, which limits direct freshwater discharge to the coastal ocean (Yang et al., 2002). As a result, the effective freshwater outflow rate remains very small (mean: ~ 0.0004 Sv; 1 Sv = 10^6 m^3 sec^{-1}). Moreover, riverine freshwater is largely confined to the surface mixed layer due to buoyancy-driven stratification, further restricting its influence on the deep-water nutrient inventory. These constraints indicate that river-derived P cannot exert a strong control on basin-scale, depth-integrated nutrient stoichiometry in the EJS.

A seasonal alternative is the intrusion of Changjiang Discharge Water (CDW) from the East China Sea, which enters the southern EJS during summer (Fig. S2) (Isobe et al., 2002). However, CDW is generally characterized by very high DIN:DIP ratios, typically ranging from 50−100 near the river mouth and inner shelf, reflecting strong N enrichment from anthropogenic inputs (Lee et al., 2009). Although the DIN:DIP ratio decreases offshore to values of ~10–20 in surface waters and < 10 in subsurface waters due to mixing and biogeochemical processing. However, because Changjiang-derived freshwater is substantially less dense than surrounding seawater, it forms a buoyant plume that remains largely restricted to the upper mixed layer rather than penetrating into deeper waters (Tseng et al., 2014). In addition, transport through the Korea Strait exhibits strong seasonal variability, with larger

inflow during summer-autumn and weaker transport during winter-spring (Takikawa et al., 1999; Taegue et al., 2002). Furthermore, the influence of CDW has likely weakened in recent decades due to declining Changjiang discharge volume (Myriokefalitakis et al., 2016), further reducing its potential contribution to basin-scale nutrient stoichiometry in the EJS. Consequently, CDW intrusion is unlikely to account for the persistent low NO_3^-:PO_4^{3-} ratios observed throughout the water column and across seasons in the EJS. Because this influence is confined to the southern surface layer (Beardsley et al., 1985) and is strongly seasonal, it cannot plausibly generate a basin-wide, persistent, depth-coherent low NO_3^-:PO_4^{3-} signal extending to 1000 m.

Second, atmospheric deposition can also contribute bioavailable P to surface waters via aerosols, mineral dust, and volcanic ash (i.e., particularly in regions influenced by volcanic activity) (Myriokefalitakis et al., 2016). The EJS lies downwind of heavily industrialized and densely populated areas of Northeast Asia, making it a potential recipient of anthropogenic emissions (Seo and Kim, 2023). However, recent studies have shown that since the 1980s, atmospheric deposition has led to a substantial increase in reactive N in the upper EJS ($\sim$0.24 μmol kg^{-1} yr^{-1}), resulting in a measurable rise in NO_3^- relative to PO_4^{3-} concentrations (Kim et al., 2014). Thus, atmospheric deposition acts in the opposite direction to a P-driven explanation, enhancing surface N excess and increasing NO_3^-:PO_4^{3-} ratios rather than lowering them, and therefore cannot sustain low ratios beyond the surface or over long time-scales.

Third, seawater–crust interactions, particularly at hydrothermal vents under low-oxygen and high-temperature conditions, are known to release PO_4^{3-} into the water column (McManus et al., 1997). However, no hydrothermal activity has been identified within the EJS.

Fourth, sedimentary P release represents a potential internal source under reducing conditions. However, sediment studies in the EJS indicate that P is largely retained through burial and adsorption processes, with phosphate released during early diagenesis efficiently scavenged by iron oxides under oxic conditions (Cha et al., 2005). As a result, sediment-derived P is unlikely to be released in sufficient quantities to influence the overlying water column at basin scale, particularly across the full depth range.

Taken together, none of these sources—riverine, lateral (CDW), atmospheric, hydrothermal, or sedimentary—satisfy the fundamental requirement of sustaining a basin-wide, depth-coherent low NO_3^-:PO_4^{3-} signal. Enhanced phosphorus supply can therefore be excluded, leaving N loss as the only mechanism consistent with the observations.

3.54 Dual-scale feedbacks on the NO_3^-: PO_4^{3-} ratio

~~Our findings provide insight into the evolving biogeochemistry of the EJS under anthropogenic and climatic pressures that operate on distinct timescales and depth domains (Fig. 4).~~The anomalously low N:P signature of the EJS emerges from processes that unfold on markedly different temporal and vertical scales. Signals at the ocean surface adjust rapidly to external perturbations, whereas changes in the interior evolve more slowly, integrating over longer timescales. This separation in timescales governs both the present expression of the N:P balance and its potential future trajectory under ongoing environmental change. Here, we distinguish short-term surface responses from the longer-term reorganization of the subsurface reactive N inventory.

In the surface layer, external N supply has increasingly been shaped by atmospheric N deposition rather than in situ N_2 fixation. Basin-scale analyses show a detectable rise of upper-ocean NO_3^- across the NPO, with the fastest increase in excess N relative to P (i.e., referred to as N^*) occurring in the EJS (~~~~0.24 μmol kg^{-1} yr^{-1}) and a systematic decrease eastward with distance from Asian source regions—patterns consistent with the magnitude and distribution of atmospheric N deposition (Kim et al., 2014; Lee et al., 2020). This has produced an N-replete surface environment (i.e., a shift from N-limitation to P-limitation; see ~~Supplementary~~ Fig. S4). ~~The~~Because this anthropogenic signal emerged without concurrent changes in dissolved O_2 or P and does not require an increase in N_2 fixation, indicating atmospheric N deposition as the primary driver of the stoichiometric shift. While our data do not directly attribute the higher NO_3^-:PO_4^{3-} ratios in surface waters relative to deeper layers to atmospheric inputs, our observations clearly reveal a vertically structured stoichiometry gradient (Fig. 1C). Given that external N inputs are primarily confined to the surface layer, continued atmospheric deposition would be expected to further strengthen this surface–deep vertical contrast over time. As external N supply increases, the relative importance of in situ N_2 fixation is likely reduced, reinforcing the role of atmospheric inputs in regulating surface N availability. Because this external forcing is largely confined to the surface layer, its impact is inherently depth-dependent. ~~As deposition continues, the surface NO_3^-:PO_4^{3-} ratio is likely to increase on shorter timescales, establishing a positive feedback that reinforces surface NO_3^- accumulation.~~

In contrast~~deep waters~~, changes in deep waters reflect longer-term ventilation dynamics~~climate driven processes appear to be reshaping nutrient dynamics over longer timescales~~. Historically, the EJS was ventilated by winter deep convection that renewed oxygen-rich bottom waters; however, tracer and hydrographic records indicate a mode shift in ventilation, from deep convection to predominantly intermediate-depth convection (~700–2000 m) (Gamo, 1999; Gamo et al., 2001; Kang et al., 2003). Over the same period, deep-water DO decreased by up to ~20 μM, and the oxygen-minimum layer deepened from a few hundred meters in the late 1960s to >1500 m by the 1990s—consistent with surface warming, reduced winter cooling, and strengthened stratification that reroutes ventilation to shallower layers (Kang et al., 2004; Kim et al., 2001). Although an exceptionally cold winter in 2000–2001 briefly re-initiated bottom-water renewal, the event was small and transient (≈0.03% of historical annual formation) (Kim et al., 2002; Talley et al., 2003). Forward modeling with a moving-boundary box framework further suggests that present bottom waters will be replaced by deep/central waters by ~2040, implying continued long-term deoxygenation~~oxygen decline~~ (Kang et al., 2003; Kang et al., 2004). Although these changes do not imply the development of basin-scale anoxia, the gradual decline in oxygen and reduced ventilation may influence the balance of the reactive N inventory over decadal timescales. In particular, declining oxygen concentrations and longer water-mass residence times may increase the relative importance of NO_3^- reduction pathways operating within localized low-oxygen microenvironments, such as particle-associated niches. Over decadal timescales, the cumulative effect of these processes could gradually reduce the deep-water N inventory, consistent with the observed decline in ~~deep~~ NO_3^-:PO_4^{3-} ratios (e.g., NO_3^-:$PO_4^{3-}{}_{1999}$ = 13.0 > NO_3^-:$PO_4^{3-}{}_{2021}$ = 12.6; see ~~Supplementary~~ Fig. S4).

~~Together, these dual-scale feedbacks—surface N enrichment driven by anthropogenic N deposition (short-term: increasing NO_3^-:PO_4^{3-} ratio in the upper waters) and subsurface N removal associated with climate-driven deoxygenation (long-term: decreasing NO_3^-:PO_4^{3-} ratio in the deep waters)—may create a vertically stratified NO_3^-:PO_4^{3-} regime in the future EJS.~~ Taken together, these observations support a dual-scale framework in which short-term surface N enrichment driven by atmospheric

deposition increases NO_3^-:PO_4^{3-} ratios, while longer-term adjustments in the subsurface N inventory—linked to ventilation changes and microenvironment-mediated N loss—act in the opposite direction. These processes operate without requiring the onset of anoxia and instead reflect shifts in the balance of N cycling pathways across temporal and vertical scales. Given this dual sensitivity to atmospheric forcing and ventilation dynamics, the EJS may serve as a sentinel system for detecting biogeochemical responses ~~in~~to ongoing ~~other marine~~ environmental changes~~.~~

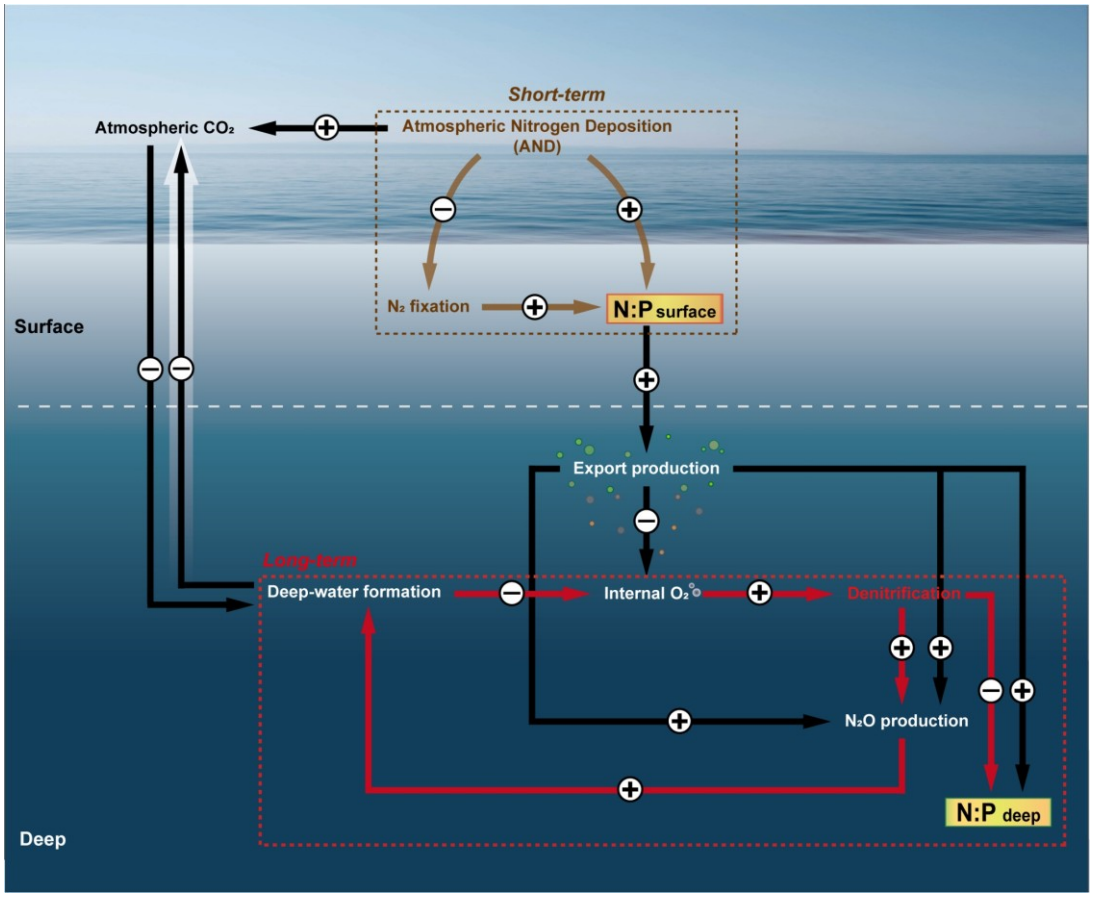

Figure 54: Conceptual schematic summarizing external drivers influencing the NO_3^-:PO_4^{3-} ratio in the East/Japan Sea. The schematic illustrates a simplified pathway showing the sequential influences on the NO_3^-:PO_4^{3-} ratio, driven by two key external factors: atmospheric N deposition, acting as a short-term driver (brown dashed box), and climate-induced suppression of deep-water formation, representing a long-term driver (red dashed box). Arrows indicate potential intermediate links among processes. A plus sign (+) denotes enhancement, whereas a minus sign (–) indicates suppression of the process.

3.~~5~~6 Caveats and Future directions

While our study provides a plausible explanation for the anomalously low NO_3^-:PO_4^{3-} ratio in the East/Japan Sea (EJS), several caveats must be emphasized. First, our inference of bacterially mediated N loss is derived from genetic and taxonomic evidence rather than direct rate measurements. Although the high relative abundances of N-reducing genes and affiliated taxa suggest the

potential for active denitrification, the actual magnitude of N loss remains unconstrained. Future studies should therefore incorporate direct process-rate determinations, such as N isotope tracer incubations, in situ microsensor profiling within sinking aggregates, and sediment-trap experiments to quantify particle-associated N loss more precisely. Second, the spatiotemporal variability of oxygen-depleted microenvironments in the EJS remains poorly characterized. The formation, persistence, and turnover of such microzones likely vary with aggregate composition, particle flux intensity, and seasonal productivity, yet these dynamics were not resolved here. High-resolution time-series observations that integrate biological, chemical, and physical measurements will be essential to capture these short-lived but biogeochemically significant microenvironments. Finally, the EJS should be considered not only a regional anomaly but also a testbed for broader climate–biogeochemistry feedbacks. Comparative studies across other well-oxygenated marginal seas and open-ocean settings are urgently needed to evaluate whether particle-associated microenvironments constitute a widespread and underappreciated sink for fixed N. Such efforts, combining multi-omics approaches with direct rate measurements and coupled physical–biogeochemical models, will be critical for predicting how anthropogenic nutrient inputs and climate-driven deoxygenation jointly reshape the global N cycle.

4 Summary and Conclusions

The EJS, which is a well-oxygenated marginal sea, exhibits an anomalously low NO_3^-:PO_4^{3-} ratio (12.6:1), deviating from the canonical Redfield ratio (16:1). External P inputs are insufficient to explain this anomaly. Instead, N-reducing genes and taxa suggest that bacterially mediated N loss is a plausible contributing factor, potentially occurring in particle-associated microenvironments (i.e., oxygen-depleted microzones in sinking aggregates). We propose a dual-scale feedback: short-term anthropogenic N deposition enriches surface waters (i.e., increasing NO_3^-:PO_4^{3-} ratio in the upper waters), while longer-term climate-driven deoxygenation could promote subsurface N loss (i.e., decreasing NO_3^-:PO_4^{3-} ratio in the deep waters). This combination may result in a vertically stratified stoichiometric regime in the future EJS. The EJS thus serves as a sentinel system, illustrating how concurrent human and climatic pressures may reshape marine nutrient cycling and offering insight into future changes in global ocean biogeochemistry.

Authorship contribution statement

Hyo-Ryeon Kim: Conceptualization, Software, Writing - Original Draft, Visualization. **Jae-Hyun Lim:** Conceptualization, Validation, Investigation. **Hae-Kun Jun:** Conceptualization, Validation, Investigation, Data curation. **Jeong-Min Shim:** Conceptualization, Validation, Investigation. **Ju-Hyoung Kim:** Conceptualization, Validation, Writing - Review & Editing. **Seo-Young Kim:** Software, Validation. **Il-Nam Kim:** Conceptualization, Writing - Original Draft, Validation, Supervision.

Funding

This study was supported by National Research Foundation of Korea (NRF) funded by Korean government (MSIT) (NRF-2022R1A2C1008475) and National Institute of Fisheries Science (NIFS), MOF, Korea (R2025015).

Declaration of competing interest

The authors declare that they have no known competing financial interests or personal relationships that could have appeared to influence the work reported in this paper.

Acknowledgements

We would like to thank the captain and crew members of the R/V Tamgu 3 for their endless support during the 2021 cruises.

Data availability

Data will be made available on request.

~~Appendix A.~~ Supplementary materials

The supplementary materials (Figs. S1–4 and Table S1–3) are found in the submitted files.

References

Alldredge, A. L., and Cohen, Y.: Can microscale chemical patches persist in the sea? Microelectrode study of marine snow, fecal pellets, *Science*, **235**(4789), 689–691, https://doi.org/10.1126/science.235.4789.689, 1987.

Alldredge, A. L., and Silver, M. W.: Characteristics, dynamics and significance of marine snow, *Prog. Oceanogr.*, **20**(1), 41–82, https://doi.org/10.1016/0079-6611(88)90053-5, 1988.

Arrigo, K. R.: Marine microorganisms and global nutrient cycles, *Nature*, **437**(7057), 349–355. https://doi.org/10.1038/nature04159, 2005.

Bao, X. G., Chong, P. F., He, C., Wang, X. Y., Zhang, F., Tan, B. B., and Lou, K. X.: *Bacillus tequilensis* S40 inoculation alleviates salt stress by modifying bacterial community structure and regulating elemental cycling rhizosphere of *Reaumuria soongorica*, *BMC Plant Biol.*, **25**, 1251, https://doi.org/10.1186/s12870-025-07122-4, 2025.

Biao, Z., Jiajun, L., Yansong, L., Xiangyu, G., Lihua, W., Guangshuai, Z., Dandan, W., Yuntao, X., and Rujia, L.: Characteristics of microbial communities and nitrogen cycling in large and small estuaries. *Mar. Environ. Res.*, 107283, https://doi.org/10.1016/j.marenvres.2025.107283, 2025.

Bianchi, D., Weber, T. S., Kiko, R., and Deutsch, C.: Global niche of marine anaerobic metabolisms expanded by particle microenvironments, *Nat. Geosci.*, **11**(4), 263–268, https://doi.org/10.1038/s41561-018-0081-0, 2018.

Broman, E., Zilius, M., Samuiloviene, A., Vybernaite-Lubiene, I., Politi, T., Klawonn, I., Voss, M., Nascimento, F. J. A., and Bonaglia, S.: Active DNRA and denitrification in oxic hypereutrophic waters. *Water Res.*, **194**, 116954, https://doi.org/10.1016/j.watres.2021.116954, 2021.

Cha, H. J., Lee, C. B., Kim, B. S., Choi, M. S., and Ruttenberg, K. C.: Early diagenetic redistribution and burial of phosphorus in the sediments of the southwestern East Sea (Japan Sea). *Mar. Geol.*, **216**(3), 127–143, https://doi.org/10.1016/j.margeo.2005.02.001, 2005.

Ciccarese, D., Tantawi, O., Zhang, I. H., Plata, D., and Babbin, A. R.: Microscale dynamics promote segregated denitrification in diatom aggregates sinking slowly in bulk oxygenated seawater, *Commun. Earth Environ.*, **4**(1), 275, https://doi.org/10.1038/s43247-023-00935-x, 2023.

Cram, J. A., Chow, C. E. T., Sachdeva, R., Needham, D. M., Parada, A. E., Steele, J. A., and Fuhrman, J. A.: Seasonal and interannual variability of the marine bacterioplankton community throughout the water column over ten years. *ISME J.*, **9**(3), 563–580, https://doi.org/10.1038/ismej.2014.153, 2015.

Dai, X., Chen, M., Wan, X., Tan, E., Zeng, J., Chen, N., Kao, S. J, and Zhang, Y.: Potential contributions of nitrifiers and denitrifiers to nitrous oxide sources and sinks in China's estuarine and coastal areas. *Biogeosciences*, **19**(16), 3757–3773, https://doi.org/10.5194/bg-19-3757-2022, 2022.

Delmont, T. O., Pierella Karlusich, J. J., Veseli, I., Fuessel, J., Eren, A. M., Foster, R. A., Bowler, C., Wincker, P., Pelletier, E.: Heterotrophic bacterial diazotrophs are more abundant than their cyanobacterial counterparts in metagenomes covering most of the sunlit ocean. *ISME J.*, **16**(4), 927–936, https://doi.org/10.1038/s41396-021-01135-1, 2022.

Desjardins, P., and Conklin, D.: Nanodrop Microvolume Quantitation of Nucleic Acids, *J Vis Exp.*, (45):2565, https://doi.org/10.3791/2565, 2010.

Deutsch, C., Gruber, N., Key, R. M., Sarmiento, J. L., and Ganachaud, A.: Denitrification and N_2 fixation in the Pacific Ocean, *GLOBAL BIOGEOCHEM CY.*, **15**(2), 483–506, https://doi.org/10.1029/2000GB001291, 2001.

Ding, C., and Sun, J.: The potential contribution of microbial communities to carbon fixation and nitrogen cycle in the Eastern Indian Ocean. *Mar. Environ. Res.*, 207, 107056, https://doi.org/10.1016/j.marenvres.2025.107056, 2025.

Edgar, R. C.: Search and clustering orders of magnitude faster than BLAST. *Bioinform.*, **26**(19), 2460–2461, https://doi.org/10.1093/bioinformatics/btq461, 2010.

Fontanez, K. M., Eppley, J. M., Samo, T. J., Karl, D. M., and DeLong, E. F.: Microbial community structure and function on sinking particles in the North Pacific Subtropical Gyre. *Front. Mar. Sci.*, **6**, 469. https://doi.org/10.3389/fmicb.2015.00469, 2015.

Fuhrman, J. A., Comeau, D. E., Hagström, A., and Chan, A. M.: Extraction from Natural Planktonic Microorganisms of DNA Suitable for Molecular Biological Studies, *Appl. Environ. Microbiol.*, **54**(6), 1426–1429, https://doi.org/10.1128/aem.54.6.1426-1429.1988, 1988.

Fujii, N., Kuroda, K., Narihiro, T., Aoi, Y., Ozaki, N., Ohashi, A., and Kindaichi, T.: Metabolic potential of the superphylum Patescibacteria reconstructed from activated sludge samples from a municipal wastewater treatment plant, *M&E.*, **37**(3), ME22012, https://doi.org/10.1264/jsme2.ME22012, 2022.

Gamo, T.: Global warming may have slowed down the deep conveyor belt of a marginal sea of the northwestern Pacific: Japan Sea, *Geophys. Res. Lett.*, **26**(20), 3137–3140, https://doi.org/10.1029/1999GL002341, 1999.

Gamo, T., Momoshima, N., and Tolmachyov, S.: Recent upward shift of the deep convection system in the Japan Sea, as inferred from the geochemical tracers tritium, oxygen, and nutrients, *Geophys. Res. Lett.*, **28**(21), 4143–4146, https://doi.org/10.1029/2001GL013367, 2001.

Gruber, N.: The marine nitrogen cycle: overview and challenges, in: Nitrogen Marine Environment, edited by: Douglas, G. C., Deborah, A. B., Margaret, R. M., and Edward, J. C., Elsevier Science & Technology, Oxford, UK, 1–50, ISBN: 978–0–12–372522–6, 2008.

Gruber, N., and Sarmiento, J. L.: Global patterns of marine nitrogen fixation and denitrification, *GLOBAL BIOGEOCHEM CY.*, **11**(2), 235–266, https://doi.org/10.1029/97GB00077, 1997.

Hallin, S., Philippot, L., Löffler, F. E., Sanford, R. A., and Jones, C. M.: Genomics and ecology of novel N_2O-reducing microorganisms. *Trends Microbiol.*, **26**(1), 43–55, https://doi.org/10.1016/j.tim.2017.07.003, 2018.

Isobe, A., Ando, M., Watanabe, T., Senjyu, T., Sugihara, S., and Manda, A.: Freshwater and temperature transports through the Tsushima-Korea Straits, *J. Geophys. Res. Oceans.*, **107**(C7), 2–1, https://doi.org/10.1029/2000JC000702, 2002.

Kang, D. J., Park, S., Kim, Y. G., Kim, K., and Kim, K. R.: A moving-boundary box model (MBBM) for oceans in change: An application to the East/Japan Sea, *Geophys. Res. Lett.*, **30**(6), https://doi.org/10.1029/2002GL016486, 2003.

Kang, D. J., Kim, J. Y., Lee, T., and Kim, K. R.: Will the East/Japan Sea become an anoxic sea in the next century?, *Mar. Chem.*, **91**(1–4), 77–84, https://doi.org/10.1016/j.marchem.2004.03.020, 2004.

Kim, I. N., Min, D. H., and Lee, T.: Deep Nitrate Deficit Observed in the Highly Oxygenated East/Japan Sea and Its Possible Cause, *Terr. Atmos. Ocean. Sci.* **23**, 671–683, https://doi.org/10.3319/TAO.2012.08.11.01(Oc), 2012.

Kim, T. H., and Kim, G.: Changes in seawater N: P ratios in the northwestern Pacific Ocean in response to increasing atmospheric N deposition: Results from the East (Japan) Sea. *Limnol. Oceanogr.*, **58**(6), https://doi.org/10.4319/lo.2013.58.6.1907, 1907–1914, 2013.

Kim, I. N., Min, D. H., and Macdonald, A. M.: Water column denitrification rates in the oxygen minimum layer of the Pacific Ocean along 32S, *Global Biogeochem Cy.*, **27**(3), 816–827, https://doi.org/10.1002/gbc.20070, 2013.

Kim, I. N., Lee, K., Gruber, N., Karl, D. M., Bullister, J. L., Yang, S., and Kim, T. W.: Increasing anthropogenic nitrogen in the North Pacific Ocean, *Science*, **346**(6213), 1102–1106, https://doi.org/10.1126/science.1258396, 2014.

Kim, I. N.: Estimating Denitrification Rates in the East/Japan Sea Using Extended Optimum Multi-Parameter Analysis, *Terr. Atmos. Ocean. Sci*, **26**, https://doi.org/10.3319/TA0.2014.09.24.01(Oc), 2015.

Kim, K., Kim, K. R., Min, D. H., Volkov, Y., Yoon, J. H., and Takematsu, M.: Warming and structural changes in the East (Japan) Sea: a clue to future changes in global oceans?, *Geophys. Res. Lett.*, **28**(17), 3293–3296, https://doi.org/10.1029/2001GL013078, 2001.

Kim, K. R., Kim, G., Kim, K., Lobanov, V., Ponomarev, V., and Salyuk, A.: A sudden bottom-water formation during the severe winter 2000–2001: The case of the East/Japan Sea, *Geophys. Res. Lett.*, **29**(8), 75–1, https://doi.org/10.1029/2001GL01449, 2002.

Klindworth, A., Pruesse, E., Schweer, T., Peplies, J., Quast, C., Horn, M., and Glöckner, F. O.: Evaluation of general 16S ribosomal RNA gene PCR primers for classical and next-generation sequencing-based diversity studies, *Nucl. Acids Res.*, **41**(1), e1–e1, https://doi.org/10.1093/nar/gks808, 2013.

Kong, L. F., Yan, K. Q., Xie, Z. X., He, Y. B., Lin, L., Xu, H. K., Liu, S. Q., and Wang, D. Z.: Metaproteomics reveals similar vertical distribution of microbial transport proteins in particulate organic matter throughout the water column in the Northwest Pacific Ocean. *Front. Microbiol*., **12**, 629802. https://doi.org/10.3389/fmicb.2021.629802, 2021.

Kozich, J. J., Westcott, S. L., Baxter, N. T., Highlander, S. K., and Schloss, P. D.: Development of a dual-index sequencing strategy and curation pipeline for analyzing amplicon sequence data on the MiSeq Illumina sequencing platform. *Appl. Environ. Microbiol.,* **79**(17), 5112–5120, https://doi.org/10.1128/AEM.01043-13, 2013.

Kwak, J. H., Lee, S. H., Park, H. J., Choy, E. J., Jeong, H. D., Kim, K. R., and Kang, C. K.: Monthly measured primary and new productivities in the Ulleung Basin as a biological "hot spot" in the East/Japan Sea, *Biogeosciences*, **10**(7), 4405–4417, https://doi.org/10.5194/bg-10-4405-2013, 2013.

Lee, K., Lee, E., and Lee, C. H.: Anthropogenic Perturbations of the Carbon and Nitrogen Cycles in the East Sea (Sea of Japan), in: Changing Asia-Pacific Marginal Seas, edited by: Chen, C. T., and Guo, X., 87–103 pp., Springer, Singapore, https://doi.org/10.1007/978-981-15-4886-4_6, 2020.

Lee, J. Y., Kang, D. J., Kim, I. N., Rho, T., Lee, T., Kang, C. K., and Kim, K. R.: Spatial and temporal variability in the pelagic ecosystem of the East Sea (Sea of Japan): a review. *J. Mar. Syst.*, **78**(2), 288–300, https://doi.org/10.1016/j.jmarsys.2009.02.013, 2009.

Lee, T., and Rho, T. K.: Seawater N/P ratio of the East Sea. *J. Korean Soc. Oceanogr*., **20**(4), 199–205, http://dx.doi.org/10.7850/jkso.2015.20.4.199, 2015.

Li, Y., Jing, H., Xia, X., Cheung, S., Suzuki, K., and Liu, H.: Metagenomic insights into the microbial community and nutrient cycling in the western subarctic Pacific Ocean. *Front. Microbiol.*, **9**, 623, https://doi.org/10.3389/fmicb.2018.00623, 2018.

Loisel, H., Nicolas, J. M., Deschamps, P. Y., and Frouin, R.: Seasonal and inter - annual variability of particulate organic matter in the global ocean. *Geophys. Res. Lett.*, **29**(24), 49–1, https://doi.org/10.1029/2002GL015948, 2002.

Lüke, C., Speth, D. R., Kox, M. A., Villanueva, L., and Jetten, M. S.: Metagenomic analysis of nitrogen and methane cycling in the Arabian Sea oxygen minimum zone, *PeerJ*, 4, e1924, https://doi.org/10.7717/peerj.1924, 2016.

Marchant, H. K., Mohr, W., and Kuypers, M. M.: Recent advances in marine N-cycle studies using 15N labeling methods, *Curr. Opin. Biotech.*, **41**, 53–59, https://doi.org/10.1016/j.copbio.2016.04.019, 2016.

Martiny, A., Pham, C., Primeau, F. Brugt, J., Moore, J., Levin, S., and Lomas, M.: Strong latitudinal patterns in the elemental ratios of marine plankton and organic matter. *Nature Geosci*, **6**, 279–283, https://doi.org/10.1038/ngeo1757, 2013.

McManus, J., Berelson, W. M., Coale, K. H., Johnson, K. S., and Kilgore, T. E.: Phosphorus regeneration in continental margin sediments, *Geochim. Cosmochim. Acta.*, **61**(14), 2891–2907, https://doi.org/10.1016/S0016-7037(97)00138-5, 1997.

Moreno-Vivián, C., Cabello, P., Martínez-Luque, M., Blasco, R., and Castillo, F.: Prokaryotic nitrate reduction: molecular properties and functional distinction among bacterial nitrate reductases. *J. Bacteriol.*, **181**(21), 6573–6584, https://doi.org/10.1128/jb.181.21.6573-6584.1999, 1999.

Myriokefalitakis, S., Nenes, A., Baker, A. R., Mihalopoulos, N., and Kanakidou, M.: Bioavailable atmospheric phosphorous supply to the global ocean: a 3-D global modeling study, *Biogeosciences*, **13**, 6519–6543, https://doi.org/10.5194/bg-13-6519-2016, 2016.

Na, T., Thamdrup, B., Kim, B., Kim, S. H., Vandieken, V., Kang, D. J., and Hyun, J. H.: N_2 production through denitrification and anammox across the continental margin (shelf–slope–rise) of the Ulleung Basin, East Sea, *Limnol. Oceanogr.*, **63**(S1), S410–S424, https://doi.org/10.1002/lno.10750, 2018.

Otosaka, S., Tanaka, T., Togawa, O., Amano, H., Karasev, E. V., Minakawa, M., and Noriki, S.: Deep sea circulation of particulate organic carbon in the Japan Sea, *J. Oceanogr.*, **64**(6), 911–923, https://doi.org/10.1007/s10872-008-0075-4, 2008.

Pace, N. R.: A molecular view of microbial diversity and the biosphere, *Science*, **276**(5313), 734–740, https://doi.org/10.1126/science.276.5313.734, 1997.

Pajares, S., and Ramos, R.: Processes and microorganisms involved in the marine nitrogen cycle: knowledge and gaps, *Front. Mar. Sci.*, **6**, 739, https://doi.org/10.3389/fmars.2019.00739, 2019.

Ploug, H., Kühl, M., Buchholz-Cleven, B., and Jørgensen, B. B.: Anoxic aggregates-an ephemeral phenomenon in the pelagic environment?, *Aquat. Microb. Ecol.*, **13**(3), 285–294, https://doi.org/10.3354/ame013285, 1997.

Podlesnaya, G. V., Potapov, S. A., Krasnopeev, A. Y., Shtykova, Y. R., Tomberg, I. V., Timoshkin, O. A., and Belykh, O. I.: Diversity of denitrifying bacteria in biofilms formed on stony substrates of the lake Baikal Littoral Zone, *Microbiol.*, **89**(3), 369–373, https://doi.org/10.1134/S0026261720030133, 2020.

Quan, Q., Liu, J., Li, C., Ke, Z., and Tan, Y.: Insights into prokaryotic communities and their potential functions in biogeochemical cycles in cold seep. *Msphere*, **9**(10), e00549-24. https://doi.org/10.1128/msphere.00549-24, 2024.

Quast, C., Pruesse, E., Yilmaz, P., Gerken, J., Schweer, T., Yarza, P., Peplies, J., and Glöckner, F. O.: The SILVA ribosomal RNA gene database project: improved data processing and web-based tools, *Nucl. Acids Res.*, **41**(D1), D590–D596, https://doi.org/10.1093/nar/gks1219, 2013.

Redfield, A. C.: The biological control of chemical factors in the environment, *Am. Sci.*, **46**(3), 230A–221, http://www.jstor.org/stable/27827150, 1958.

Rocca, J. D., Hall, E. K., Lennon, J. T., Evans, S. E., Waldrop, M. P., Cotner, J. B., Nemergut, D. R., Graham, E. B., and Wallenstein, M. D.: Relationships between protein-encoding gene abundance and corresponding process are commonly assumed yet rarely observed. *ISME J.*, **9**(8), 1693–1699, https://doi.org/10.1038/ismej.2014.252, 2015.

Russell, M. V., Messer, T. L., Repert, D. A., Smith, R. L., Bartelt-Hunt, S., Snow, D. D., and Reed, A. P.: Influence of Four Veterinary Antibiotics on Constructed Treatment Wetland Nitrogen Transformation, *Toxics*, **12**(5), 346, https://doi.org/10.3390/toxics12050346, 2024.

Sayers, E. W., Beck, J., Bolton, E. E., Bourexis, D., Brister, J. R., Canese, K., Comeau, D. C., Funk, K., Kim, S., Klimke, W., Marchler-Bauer, A., Landrum, M., Lathrop, S., Lu, Z., Madden, T. L., O'Leary, N., Phan, L., Rangwala, S. H., Schneider, V. A., Skripchenko, Y., Wang, J., Ye, J., Trawick, B. W., Pruitt, K. D., and Sherry, S. T. Database resources of the national center for biotechnology information. *Nucl. Acids Res.*, **49**(D1), D10–D17. https://doi.org/10.1093/nar/gkaa892, 2021.

Seo, H., and Kim, G.: Anthropogenic iron invasion into the ocean: Results from the East Sea (Japan Sea), *ES&T*, **57**(29), 10745–10753, https://doi.org/10.1021/acs.est.3c01084, 2023.

Seung, Y. H., and Yoon, J. H.: Some features of winter convection in the Japan Sea, *J. Oceanogr.*, **51**(1), 61–73, https://doi.org/10.1007/BF02235936, 1995.

Sharma, V., Chetal, G., Taylor, T. D., and Prakash, T.: Metagenomics of the Microbial Nitrogen Cycle: Functional Assignment of Metagenomic Data: Insights for the Microbial Nitrogen Cycle, Edited by: Diana Marco, Caister Academic Press, UK, 1–15, ISBN 978-1-908230-60-7, 2014.

Starke, R., Müller, M., Gaspar, M., Marz, M., Küsel, K., Totsche, K. U., Bergen, M., and Jehmlich, N.: Candidate Brocadiales dominates C, N and S cycling in anoxic groundwater of a pristine limestone-fracture aquifer, *J Proteomics*, **152**, 153–160, https://doi.org/10.1016/j.jprot.2016.11.003, 2017.

Tang, W., Tracey, J. C., Carroll, J., Wallace, E., Lee, J. A., Nathan, L., Sun, X., Jayakumar, A., Ward, B. B.: Nitrous oxide production in the Chesapeake Bay. *Limnol. Oceanogr.*, **67**(9), 2101–2116, https://doi.org/10.1002/lno.12191, 2022.

Takikawa, T., Yoon, J. H., Hase, H., and Cho, K. D.: Monitoring of the Tsushima Current at the Tsushima/Korea Straits. *Proceedings 3rd CREAMS International Symposium*, Fukuoka, Japan, 15–18, 1999.

Talley, L. D., Lobanov, V., Ponomarev, V., Salyuk, A., Tishchenko, P., Zhabin, I., and Riser, S.: Deep convection and brine rejection in the Japan Sea, *Geophys. Res. Lett.*, **30**(4), https://doi.org/10.1029/2002GL016451, 2003.

Teague, W. J., Jacobs, G. A., Perkins, H. T., Book, J. W., Chang, K. I., and Suk, M. S.: Low-frequency current observations in the Korea/Tsushima Strait. *J. Phys. Oceanogr.*, **32**(6), 1621–1641, https://doi.org/10.1175/1520-0485(2002)032<1621:LFCOIT>2.0.CO;2, 2002.

Tseng, Y.-F., Lin, J., Dai, M., and Kao, S.-. J.: Joint effect of freshwater plume and coastal upwelling on phytoplankton growth off the Changjiang River, *Biogeosciences*, **11**, 409–423, https://doi.org/10.5194/bg-11-409-2014, 2014.

Tyrrell, T.: The relative influences of nitrogen and phosphorus on oceanic primary production. *Nature*, **400**, 525–531, https://doi.org/10.1038/22941, 1999.

Van Spanning, R. J. M., Delgado, M. J., and Richardson, D. J.: The nitrogen cycle: denitrification and its relationship to N_2 fixation, in: Nitrogen fixation in agriculture, forestry, ecology, and the environment, edited by: Werner, D., and Newton, W. E., Springer, Dordrecht, Netherlands, 277–342, https://doi.org/10.1007/1-4020-3544-6_13, 2005.

Wakeham, S. G., and Lee, C.: (1993). Production, transport, and alteration of particulate organic matter in the marine water column. In Organic Geochemistry: Principles and Applications (pp. 145–169). Boston, MA: Springer US.

Wan, X. S., Sheng, H. X., Liu, L., Shen, H., Tang, W., Zou, W., Xu, M. N., Zheng, Z., Tan, E., Chen, M., Zhang, Y., Ward, B. B., and Kao, S. J.: Particle-associated denitrification is the primary source of N_2O in oxic coastal waters, *Nat. Commun.*, **14**(1), 8280, https://doi.org/10.1038/s41467-023-43997-3, 2023.

Wang, X., Ye, C., Zhang, Z., Guo, Y., Yang, R., and Chen, S.: Effects of temperature shock on N_2O emissions from denitrifying activated sludge and associated active bacteria, *Bioresource technology,* **249**, 605–611, https://doi.org/10.1016/j.biortech.2017.10.070, 2018.

Wei, Z. S., Wang, J. B., Huang, Z. S., Xiao, X. L., Tang, M. R., Li, B. L., and Zhang, X.: Removal of nitric oxide from biomass combustion by thermophilic nitrification-aerobic denitrification combined with catalysis in membrane biofilm reactor, *Biomass Bioenergy*, **126**, 34–40, https://doi.org/10.1016/j.biombioe.2019.05.004, 2019.

Wemheuer, F., Taylor, J. A., Daniel, R., Johnston, E., Meinicke, P., Thomas, T., and Wemheuer, B.: Tax4Fun2: prediction of habitat-specific functional profiles and functional redundancy based on 16S rRNA gene sequences, *Environ. microbiome.*, **15**(1), 11, https://doi.org/10.1186/s40793-020-00358-7, 2020.

Withers, P. J. A., and Jarvie, H. P.: Delivery and cycling of phosphorus in rivers: a review, *Sci. Total Environ.*, **400**(1–3), 379–395, https://doi.org/10.1016/j.scitotenv.2008.08.002, 2008.

Wolgast, D. M., Carlucci, A. F., and Bauer, J. E.: Nitrate respiration associated with detrital aggregates in aerobic bottom waters of the abyssal NE Pacific, *Deep-Sea Res. II: Top. Stud. Oceanogr.*, **45**(4–5), 881–892, https://doi.org/10.1016/S0967-0645(98)00006-X, 1998.

Wu, M., Zhang, Z., Zhang, X., Dong, L., Liu, C., and Chen, Y.: Propionibacterium freudenreichii-Assisted approach reduces N_2O emission and improves denitrification via promoting substrate uptake and metabolism, *ES&T.*, **56**(23), 16895–16906, https://doi.org/10.1021/acs.est.2c05674, 2022.

Yanagi, T.: Water, salt, phosphorus and nitrogen budgets of the Japan Sea. *J. Oceanogr.*, **58**(6), 797–804, https://doi.org/10.1023/A:1022815027968, 2002.

Yang, H. S., Hwang, D. W., and Kim, G.: Factors controlling excess radium in the Nakdong River estuary, Korea: submarine groundwater discharge versus desorption from riverine particles, *Mar. Chem.*, **78**(1), 1–8, https://doi.org/10.1016/S0304-4203(02)00004-X, 2002.

Yamagishi, H., Yoshida, N., Toyoda, S., Popp, B. N., Westley, M. B., and Watanabe, S.: Contributions of denitrification and mixing on the distribution of nitrous oxide in the North Pacific, *Geophys. Res. Lett.*, **32**(4), https://doi.org/10.1029/2004GL021458, 2005.

Zhang, Y., Xie, X., Jiao, N., Hsiao, S. Y., and Kao, S. J.: Diversity and distribution of *amoA*-type nitrifying and *nirS*-type denitrifying microbial communities in the Yangtze River estuary. *Biogeosciences*, **11**(8), 2131–2145. https://doi.org/10.5194/bg-11-2131-2014, 2014.